Simulation of Copolymer Phase Separation in One-Dimensional Thin Liquid Films

Hidenori Yasuda*

Department of Mathematics, Josai University, Sakado, Saitama 350-0295, Japan.
Received 5 September 2011; Accepted (in revised version) 24 January 2012
Available online 10 February 2012

Abstract. This paper discusses the development of an invariant finite difference scheme to simulate the microphase separation of copolymers in one-dimensional thin liquid films. The film phenomena are modelled using two-phase shallow water equations and the Ohta–Kawasaki potential, which governs the phase separation of the copolymer. Non-positive volume fractions and spurious oscillations are eventually eliminated, in simulating the one-dimensional phase separation lamellar pattern.

1. Introduction

Phase separation of copolymer films is important for the fabrication of templates of quantum dots, nanowires, and nanopores in nanotechnology [1]. It has been shown that the phase separation of polymers is a flow phenomenon that can be modelled as a two-phase flow [2, 3]. However, the phase separation of a copolymer is qualitatively different from that of a polymer blend (a mixture of homopolymers), where the phase separation is a macroscopic phenomenon that ultimately forms a single circle [4]. A copolymer consists of two connected chemically different homopolymers, where phase separation cannot proceed on a macroscopic scale but is periodic on a microscopic scale and therefore often called microphase separation, governed by the Ohta-Kawasaki potential [5].

Microphase separation in a one-dimensional thin liquid film may be simulated by invariant finite difference schemes that highly resolve the interface region of the phase separation. However, the copolymer volume fractions do not remain positive in the later stages of some simulations, and spurious surface oscillations can be induced by conventional counter-measures. These drawbacks are addressed in this paper. The mathematical modelling is discussed in Section 2 and Section 3, the invariant finite difference scheme adopted in Section 4, and the subsequent simulations and conclusions in Section 5 and Section 6. The piecewise polynomial method (PPM) invoked is briefly discussed in the Appendix.

---

*Corresponding author. *Email address:* yasuda@math.josai.ac.jp (H. Yasuda)

2. Two-Phase Flow in the Liquid Film

2.1. Two-phase shallow water equations

The relevant one-dimensional two-phase shallow water equations are [4]

$$\frac{\partial\left(\alpha_d h\right)}{\partial t}+\frac{\partial}{\partial x}\left(\alpha_d h u_d\right)=0\,,\tag{2.1}$$

$$\frac{\partial\left(\alpha_c h\right)}{\partial t}+\frac{\partial}{\partial x}\left(\alpha_c h u_c\right)=0\,,\tag{2.2}$$

$$\frac{\partial u_d}{\partial t}+u_d\frac{\partial}{\partial x}u_d=-\frac{1}{\rho_d}\frac{\partial}{\partial x}\left(\rho_m g h\right)+\nu\frac{\partial^2}{\partial x^2}u_d+\frac{f_d}{\rho_d\alpha_d}\,,\tag{2.3}$$

$$\frac{\partial u_c}{\partial t}+u_c\frac{\partial}{\partial x}u_c=-\frac{1}{\rho_c}\frac{\partial}{\partial x}\left(\rho_m g h\right)+\nu\frac{\partial^2}{\partial x^2}u_c+\frac{f_c}{\rho_c\alpha_c}\,,\tag{2.4}$$

$$\alpha_d+\alpha_c=1\,.\tag{2.5}$$

Here x is the space coordinate and t the time, α denotes a volume fraction, u a velocity, ρ a density, f a force of phase separation, with the suffix d denoting a minor phase and c a major phase such that $\rho_m=\alpha_d\rho_d+\alpha_c\rho_c$ is the density of the mixture (the suffix m denotes the mixture), h is the height of the liquid film, g denotes gravity, and ν is the kinematic viscosity. Reference may also be made to Refs. [6,7], for detailed discussions of the shallow water approximation in the two-fluid model. The unknowns are the two volume fractions, the two velocities, and the height. The equation for the height is immediately obtained by adding Eqs. (2.1) and (2.2), and invoking Eq. (2.5).

In thin liquid films, gravity can be ignored and the pressure is *disjoining* rather than hydrostatic — i.e. thin liquid films are attracted to the substrate by the pressure caused by the van der Waals force. This disjoining pressure is [8,9]

$$\Pi=-\frac{A}{6\pi h^3}\cong-\frac{A}{6\pi h_0^3}\left(1-3\frac{h'}{h_0}\right)\,,\tag{2.6}$$

where A is the Hamaker constant of the mixture and $h=h_0+h'$, with the suffix denoting the constant state and the prime the perturbation.

We assume the Hamaker constant is approximately the same for each phase, and that the form of the relevant two-phase shallow water equations is not altered on using the disjoining pressure and replacing $\rho_m g$ by the corresponding pressure gradient $A/(2\pi h_0^4)$.

2.2. The phase separation potential

As previously mentioned, the Ohta–Kawasaki potential governs the phase separation of the copolymer, involving both short-range and long-range interactions [5]. The short-range interaction is modelled by the Ginzburg–Landau potential (as for polymer blends) but the long-range interaction is a Coulomb type, so we adopt

$$F\left(\psi\right)=F_s\left(\psi\right)+F_l\left(\psi\right)\,,\tag{2.7}$$

where

$$\psi = \alpha_d - \alpha_c \,, \tag{2.8}$$

$$F_s(\psi) = \int dx \left(-\frac{a}{2}\psi^2 + \frac{b}{4}\psi^4 + \frac{\gamma}{2}(\nabla\psi)^2 \right) \,, \tag{2.9}$$

$$F_l(\psi) = \frac{\varepsilon}{2} \int dx \int dx' G(x, x') \left(\psi(x) - \bar\psi \right) \left(\psi(x') - \bar\psi \right) \,, \tag{2.10}$$

$$-\Delta G(x, x') = \delta(x - x') \,. \tag{2.11}$$

Here F denotes the free energy, ψ is the order parameter, the suffix s denotes the short-range interaction and l the long-range interaction, $\bar\psi$ is the average of ψ, the coefficients a, b, γ and ε are all positive constants, x and x' are space coordinates, and G is a Green function.

The variation of the free energy with the order parameter gives the chemical potential

$$\mu = \mu_s + \mu_l \,, \tag{2.12}$$

where

$$\mu_s = -a\psi + b\psi^3 - \gamma\Delta\psi \,, \tag{2.13}$$

$$\mu_l = \varepsilon \int dx' G(x, x') \left(\psi(x') - \bar\psi \right) \,. \tag{2.14}$$

The assumed form for the force of phase separation is

$$f = -\rho\nabla \left(\frac{\delta F(\rho)}{\delta\rho} \right) \tag{2.15}$$

where $\delta F(\rho)/\delta\rho$ represents the variation of the free energy with density, which is the excess free energy of a test particle of the same liquid in local equilibrium and the potential energy of the test particle itself. (The force acting on the test particle is the gradient of the excess free energy.) The force per unit volume given by Eq. (2.15) may be viewed as due to ρ particles per unit volume — as discussed in a book by Kawasaki [10], one of the authors of Ref. [5]. For the two-phase flow, the forces of phase separation adopted are therefore

$$f_d = -(\rho_d\alpha_d)\nabla \left(\frac{\delta F(\psi)}{\delta\psi}\frac{\delta\psi}{\delta(\rho_d\alpha_d)} \right) = -\alpha_d\nabla\mu \,, \tag{2.16}$$

$$f_c = -(\rho_c\alpha_c)\nabla \left(\frac{\delta F(\psi)}{\delta\psi}\frac{\delta\psi}{\delta(\rho_c\alpha_c)} \right) = \alpha_c\nabla\mu \,. \tag{2.17}$$

2.3. Lamellar pattern

For the one-dimensional periodic microphase separation, a lamellar pattern, Ohta and Kawasaki [5] proposed that

$$G(x, x') = \frac{1}{L} \sum_{n=-\infty}^{+\infty}{}' \frac{1}{(2\pi n/D)^2} \exp\left(i2\pi n(x - x')/D \right) \,, \tag{2.18}$$

where the prime on the summation means the term $n = 0$ is excluded, L is the dimension of the system, and D is the period of the lamellar pattern as determined from experiment and statistical physics considerations [11]. Mathematically, there can be many periods smaller than some critical value [12].

The sum in Eq. (2.18) turns out to be a simple form. Fourier expansion of the periodic function $f(x) = x/2 - x^2/2D$, $0 \leq x < D$ yields the uniformly convergent result [13]

$$\frac{x}{2} - \frac{x^2}{2D} = \frac{D}{12} - \frac{1}{D} \sum_{n=-\infty}^{+\infty}{}' \frac{1}{(2\pi n/D)^2} \exp(i2\pi n x/D), \qquad (2.19)$$

hence the fundamental solution (2.18) is a piece-wise quadratic curve suitable for numerical computation — viz.

$$G(x, x') = \frac{D}{L} \left(\frac{(x - x')^2}{2D} - \frac{x - x'}{2} + \frac{D}{12} \right), \qquad x - x' \in [0, D). \qquad (2.20)$$

Incidentally, differentiating Eq. (2.19) twice in the distribution sense yields

$$-\frac{1}{D} + \sum_{n=-\infty}^{+\infty} \delta(x - nD) = \frac{1}{D} \sum_{n=-\infty}^{+\infty}{}' \exp(in2\pi x/D), \qquad (2.21)$$

so a series of Dirac delta-functions appears in the second-order derivative of the Ohta–Kawasaki potential.

3. Linearized order parameter equation

For the initial state, we assume the surface height h of the liquid film is constant, the velocities are small, the volume fractions are approximately uniform, and the viscosity term is negligible compared to the force of phase separation. In cases where the densities are equal ($\rho_d = \rho_c \equiv \rho$), the two-phase shallow water equations (2.1)-(2.4) with chemical potentials defined by Eqs. (2.12)–(2.14) then reduce to

$$\frac{\partial \alpha_d}{\partial t} + \frac{\partial}{\partial x}(\alpha_d u_d) = 0, \qquad (3.1)$$

$$\frac{\partial \alpha_c}{\partial t} + \frac{\partial}{\partial x}(\alpha_c u_c) = 0, \qquad (3.2)$$

$$\frac{\partial (\alpha_d u_d)}{\partial t} = -\frac{\alpha_d}{\rho} \frac{\partial}{\partial x} \left(-a\psi + b\psi^3 - \gamma \frac{\partial^2 \psi}{\partial x^2} + \varepsilon \int G(x, x') \left(\psi(x') - \bar{\psi} \right) dx' \right), \quad (3.3)$$

$$\frac{\partial (\alpha_c u_c)}{\partial t} = \frac{\alpha_c}{\rho} \frac{\partial}{\partial x} \left(-a\psi + b\psi^3 - \gamma \frac{\partial^2 \psi}{\partial x^2} + \varepsilon \int G(x, x') \left(\psi(x') - \bar{\psi} \right) dx' \right), \quad (3.4)$$

$$\alpha_d + \alpha_c = 1, \qquad (3.5)$$

where higher order terms in the velocities are omitted from Eqs. (3.3) and (3.4).

Differentiating Eqs. (3.1) and (3.2) by time and then subtracting yields

$$\frac{\partial^2 \psi}{\partial t^2} + \frac{\partial^2 (\alpha_d u_d)}{\partial t \partial x} - \frac{\partial^2 (\alpha_c u_c)}{\partial t \partial x} = 0 \tag{3.6}$$

on using Eq. (2.8); and invoking Eqs. (3.3) and (3.4) in Eq. (3.6) and using Eq. (3.5),

$$\frac{\partial^2 \psi}{\partial t^2} - \frac{1}{\rho}\frac{\partial^2}{\partial x^2}\left(-a\psi + b\psi^3 - \gamma\frac{\partial^2 \psi}{\partial x^2}\right) = \frac{\varepsilon}{\rho}\int \frac{\partial^2}{\partial x^2}G(x,x')\left(\psi(x') - \bar{\psi}\right)dx', \quad (3.7)$$

on exchanging the order of differentiation and integration. From Eqs. (2.19)–(2.21), for the lamellar pattern the integral on the right-hand side of Eq. (3.7) becomes

$$\frac{\varepsilon}{\rho}\int \frac{\partial^2}{\partial x^2}G(x,x')\left(\psi(x') - \bar{\psi}\right)dx' = -\frac{\varepsilon D}{\rho L}\sum_n \left(\psi(x \pm nD) - \bar{\psi}\right), \tag{3.8}$$

where the order parameter is has the period D, each index n in the summation signifies a particular wave in the system, and the total number of such waves is L/D.

From the periodicity, the integro-differential equation (3.7) becomes

$$\frac{\partial^2 \psi}{\partial t^2} - \frac{1}{\rho}\frac{\partial^2}{\partial x^2}\left(-a\psi + b\psi^3 - \gamma\frac{\partial^2 \psi}{\partial x^2}\right) = -\frac{\varepsilon}{\rho}\left(\psi(x) - \bar{\psi}\right), \tag{3.9}$$

which yields the linearized equation

$$\frac{\partial^2 \psi'}{\partial t^2} - \frac{1}{\rho}\frac{\partial^2}{\partial x^2}\left(-a\psi' + 3b\bar{\psi}^2\psi' - \gamma\frac{\partial^2 \psi'}{\partial x^2}\right) = -\frac{\varepsilon}{\rho}\psi'(x), \tag{3.10}$$

where $\psi(x) = \bar{\psi} + \psi'(x)$ with ψ' the perturbation. Assuming $\psi'(x) = c(t)\exp(i2\pi x/D)$, Eq. (3.10) reduces to

$$\frac{d^2 c}{dt^2} = \left(\frac{1}{\rho}\left(\frac{2\pi}{D}\right)^2\left(\left(a - 3b\bar{\psi}^2\right) - \gamma\left(\frac{2\pi}{D}\right)^2\right) - \frac{\varepsilon}{\rho}\right)c. \tag{3.11}$$

The coefficient of the right-hand side (3.11) is positive for some period if

$$a - 3b\bar{\psi}^2 > 2\left(\varepsilon\gamma\right)^{1/2}, \tag{3.12}$$

when phase separation occurs. Similar results in the case of the Cahn–Hilliard equation are found in Ref. [14].

4. Invariant Finite Difference Scheme

The two-phase shallow water equations with the Ohta–Kawasaki potential are now discretised using finite differences and numerical integration. The general invariant finite difference scheme is as follows — cf. also [4].

The hyperbolic part of two-phase shallow water equations is first considered, starting from

$$\frac{(\alpha h)_i^{n+1} - (\alpha h)_i^n}{\Delta t} + \frac{(\alpha h u)_{i+1}^n - (\alpha h u)_{i-1}^n}{2\Delta x}$$

$$= \frac{U_{1,i+1/2}\left((\alpha h)_{i+1}^n - (\alpha h)_i^n\right) - U_{1,i-1/2}\left((\alpha h)_i^n - (\alpha h)_{i-1}^n\right)}{\Delta x^2}$$

$$+ \frac{V_{1,i+1/2}\left(u_{i+1}^n - u_i^n\right) - V_{1,i-1/2}\left(u_i^n - u_{i-1}^n\right)}{\Delta x^2} , \tag{4.1}$$

$$\frac{u_i^{n+1} - u_i^n}{\Delta t} + \frac{u_{i+1}^n + u_{i-1}^n}{2}\frac{u_{i+1}^n - u_{i-1}^n}{2\Delta x}$$

$$= -\frac{1}{\rho}\frac{(\rho_m g h)_{i+1}^n - (\rho_m g h)_{i-1}^n}{2\Delta x}$$

$$+ \frac{U_{2,i+1/2}\left((\alpha h)_{i+1}^n - (\alpha h)_i^n\right) - U_{2,i-1/2}\left((\alpha h)_i^n - (\alpha h)_{i-1}^n\right)}{\Delta x^2}$$

$$+ \frac{V_{2,i+1/2}\left(u_{i+1}^n - u_i^n\right) - V_{2,i-1/2}\left(u_i^n - u_{i-1}^n\right)}{\Delta x^2} , \tag{4.2}$$

where Δt is the size of the time step, Δx the width of the x-directional mesh, the suffix i denotes the x-directional mesh number, and n is the time step number. (The suffixes d and c are omitted because the finite difference scheme for the two phases is the same.) Here U_1, U_2, V_1 and V_2 are differentiable functions and $i \pm 1/2$ means the value at the half mesh.

The first differential approximations for the finite difference schemes, obtained by expanding in Taylor series and neglecting the higher order terms in Eqs. (4.1) and (4.2), are

$$\frac{\Delta t}{2}(\alpha h)_{tt} + (\alpha h)_t + (\alpha h u)_x = \left(U_1(\alpha h)_x\right)_x + \left(V_1 u_x\right)_x , \tag{4.3}$$

$$\frac{\Delta t}{2}u_{tt} + u_t + u u_x = -\frac{1}{\rho}\left(\rho_m g h\right)_x + \left(U_2(\alpha h)_x\right)_x + \left(V_2 u_x\right)_x . \tag{4.4}$$

Assuming the time and space derivatives can be exchanged, the second-order time differential is replaced with space differential terms through recursive substitution of the first differential approximation. Thus ignoring higher-order terms, we obtain

$$\frac{\Delta t}{2}\frac{\partial^2(\alpha h)}{\partial t^2}$$

$$\cong \frac{\Delta t}{2}\frac{\partial}{\partial t}\left(-\frac{\partial}{\partial x}(\alpha h u)\right) \cong \frac{\Delta t}{2}\frac{\partial}{\partial x}\left(-u\frac{\partial}{\partial t}(\alpha h) - \alpha h\frac{\partial}{\partial t}u\right)$$

$$\cong \frac{\Delta t}{2}\left(\frac{\partial}{\partial x}\left(uu\frac{\partial}{\partial x}(\alpha h)\right) + 2\frac{\partial}{\partial x}\left(\alpha h u\frac{\partial}{\partial x}u\right) + \frac{1}{\rho}\frac{\partial}{\partial x}\left(\alpha h\frac{\partial}{\partial x}\rho_m g h\right)\right) , \tag{4.5}$$

$$\frac{\Delta t}{2}\frac{\partial^2 u}{\partial t^2} \cong \frac{\Delta t}{2}\frac{\partial}{\partial t}\left(-\frac{\partial}{\partial x}\left(\frac{u^2}{2}\right) - \frac{1}{\rho}\frac{\partial}{\partial x}(\rho_m g h)\right)$$

$$\cong -\frac{\Delta t}{2}\frac{\partial}{\partial x}\left(u\frac{\partial}{\partial t}u + \frac{1}{\rho}\frac{\partial}{\partial t}(\rho_m g h)\right)$$

$$\cong \frac{\Delta t}{2}\left(\frac{\partial}{\partial x}\left(uu\frac{\partial}{\partial x}u\right) + \frac{1}{\rho}\frac{\partial}{\partial x}\left(u\frac{\partial}{\partial x}\rho_m g h\right) + \frac{1}{\rho}\frac{\partial^2}{\partial x^2}(\rho_m u_m g h)\right), \qquad (4.6)$$

where $\rho_m u_m = \alpha_d \rho_d u_d + \alpha_c \rho_c u_c$ is the velocity of the mixture. The third term on the right-hand side of Eq. (4.6) is obtained by multiplying Eq. (4.1) by the density and adding both phases — i.e. by invoking the mass conservation of the mixture.

The invariant finite difference scheme of the two-phase shallow water equations is then constructed from Eqs. (4.5) and (4.6) — viz.

$$\frac{(\alpha h)_i^{n+1} - (\alpha h)_i^n}{\Delta t} + \frac{(\alpha h u)_{i+1}^n - (\alpha h u)_{i-1}^n}{2\Delta x}$$

$$= \frac{\Delta t}{2}\left(u_{i+1/2}^n u_{i+1/2}^n \left((\alpha h)_{i+1}^n - (\alpha h)_i^n\right) - u_{i-1/2}^n u_{i-1/2}^n \left((\alpha h)_i^n - (\alpha h)_{i-1}^n\right)\right)/\Delta x^2$$

$$+ \Delta t \left(u_{i+1/2}^n (\alpha h)_{i+1/2}^n \left(u_{i+1}^n - u_i^n\right) - u_{i-1/2}^n (\alpha h)_{i-1/2}^n \left(u_i^n - u_{i-1}^n\right)\right)/\Delta x^2$$

$$+ \frac{\Delta t}{2}\frac{1}{\rho}\left((\alpha h)_{i+1/2}^n \left((\rho_m g h)_{i+1}^n - (\rho_m g h)_i^n\right) - (\alpha h)_{i-1/2}^n \left((\rho_m g h)_i^n - (\rho_m g h)_{i-1}^n\right)\right)/\Delta x^2, \qquad (4.7)$$

$$\frac{u_i^{n+1} - u_i^n}{\Delta t} + \frac{u_{i+1}^n + u_{i-1}^n}{2}\frac{u_{i+1}^n - u_{i-1}^n}{2\Delta x}$$

$$= -\frac{1}{\rho}\frac{(\rho_m g h)_{i+1}^n - (\rho_m g h)_{i-1}^n}{2\Delta x}$$

$$+ \frac{\Delta t}{2}\left(u_{i+1/2}^n u_{i+1/2}^n \left(u_{i+1}^n - u_i^n\right) - u_{i-1/2}^n u_{i-1/2}^n \left(u_i^n - u_{i-1}^n\right)\right)/\Delta x^2$$

$$+ \frac{\Delta t}{2\rho}\left(u_{i+1/2}^n \left((\rho_m g h)_{i+1}^n - (\rho_m g h)_i^n\right) - u_{i-1/2}^n \left((\rho_m g h)_i^n - (\rho_m g h)_{i-1}^n\right)\right)/\Delta x^2$$

$$+ \frac{\Delta t}{2\rho}\left((\rho_m g h u_m)_{i+1}^n - 2(\rho_m g h u_m)_i^n + (\rho_m g h u_m)_{i-1}^n\right)/\Delta x^2. \qquad (4.8)$$

The nonlinear scheme of Eqs. (4.7) and (4.8) is second-order in both time and space. Such invariant finite difference schemes were developed by Russian researchers and are related to transformation group theory [15, 16], and the first differential approximation (original Russian terminology) has been called a modified equation [17]. Further, the U_1, U_2, V_1 and V_2 can be regarded as an extension of a tensor viscosity [18]. Finally, Eq. (2.5) is discretised as

$$(\alpha_d)_i^{n+1} + (\alpha_c)_i^{n+1} = 1, \qquad (4.9)$$

in order to calculate $(\alpha h)_i^{n+1}$, u_i^{n+1} from Eqs. (4.7) and (4.8); and then adding $(\alpha h)_i^{n+1}$ of the major and minor phase provides the height h_i^{n+1} using Eq. (4.9), and hence the α_i^{n+1}.

In the simulations, the viscous term

$$+\nu\left(u_{i+1}^n - 2u_i^n + u_{i-1}^n\right)/\Delta x^2 \tag{4.10}$$

is usually included in the velocity equation (4.8). As previously discussed, the chemical potential defined by Eqs. (2.16) and (2.17) plays the same role as the gravitational potential in the velocity equations. Further, the discretisation is performed using the term $\left(\rho_m gh \pm \mu\right)$, instead of the term $\left(\rho_m gh\right)$ where the potential term appears, and the chemical potential is discretised as

$$
\begin{aligned}
\mu_i =&-a\psi_i + b\psi_i^3 - \gamma\frac{\psi_{i+1} - 2\psi_i + \psi_{i-1}}{\Delta x^2} + \varepsilon \int G\left(x_i, x'\right)\left(\psi\left(x'\right) - \bar{\psi}\right)dx' \\
=&-a\psi_i + b\psi_i^3 - \gamma\frac{\psi_{i+1} - 2\psi_i + \psi_{i-1}}{\Delta x^2} + \frac{\varepsilon D}{L}\sum_n \int_0^D G\left(x_i, x'\right)\left(\psi\left(x' \pm nD\right) - \bar{\psi}\right)dx',
\end{aligned}
\tag{4.11}
$$

and the trapezoidal rule is used for the numerical integration of the long-range interaction — i.e.

$$\int_0^D G\left(x_i, x'\right)\left(\psi\left(x' - nD\right) - \bar{\psi}\right)dx' \cong \sum_{j=i}^{i+D/\Delta x}\left(G\left(x_i, x_j\right)\left(\psi\left(x_j \pm nD\right) - \bar{\psi}\right)\right)w_{j-i}\Delta x. \tag{4.12}$$

Weights adopted are $w_{j-i} = 0.5$ at the end points of the integration region and $w_{j-i} = 1.0$ at the other points, and the order parameter is assumed to be periodic outside the system.

5. Numerical Simulations

5.1. Calculation of lamellar patterns

The simulations are performed using the invariant scheme discussed in Section 4, using the following parameters: space mesh width $\Delta x = 1.0$; dimension of the system 100.0; constants of the short-range interaction a, b, γ all 1.0; constant of the long-range interaction $\varepsilon = 0.1$; period of the lamellar pattern $D = 20.0$; kinematic viscosity $\nu = 100.0$; disjoining pressure Hamaker constant $A = 1000.0$; densities of both phases 1.0; and for the initial condition, the film thickness is 1.0, the velocities 0.0, the volume fractions of both phases are 0.5, and the maximum 5% perturbation period 20.0 is added. The time step width is 10^{-5}, small enough to satisfy the Courant–Friedrichs–Lewy condition. The boundary condition is periodic for the volume fractions, velocities, and surface height (the unit is arbitrary). However, the force of phase separation in the interface region is large, which is a source of stiffness.

In the corresponding simulation, the initial fluctuation continues until around the time $t = 150$. The lamellar pattern then emerges from the initial fluctuation and develops until approximately $t = 800$. The volume fractions and surface height at time 700 are shown
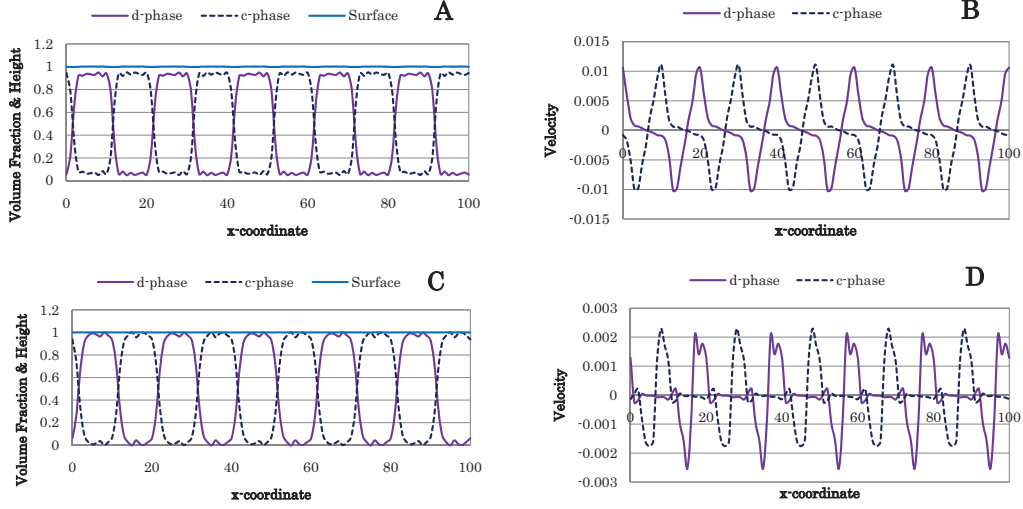
Figure 1: Phase separation in the liquid film calculated using the invariant finite difference scheme: A, volume fractions and surface height at time 700; B, velocities at time 700; C, volume fractions and surface height at time 1300; and D, velocities at time 1300.

in Fig. 1A, and the velocities in Fig. 1B. The minimum value of fractions at $t = 700$ is 0.0495, and the total variation of the surface is 0.150. The volume fractions suffer from the Gibbs oscillation, but the interface regions are highly resolved. After the lamellar pattern develops, its modulation continues and the phase separation occurs in the later stages. The volume fractions and surface height at $t = 1300$ are shown in Fig. 1C, and the velocities in Fig. 1D. The surface of the liquid film is flat, and trains of dry beds and wet beds of each phase appear repeatedly. The minimum of the volume fractions is -0.0017, so the positivity of the volume fraction is violated, although the time step width is very small. The overall surface height variation is 0.099.

The surface in the steady state is flat outside interface regions, where the surface height varies to compensate the energy of phase separation [20]. The total variation of the surface is approximately 0.005. For the dry bed regions in the ground state, the volume fraction becomes 0 near the double well of the short-range interaction in Eq. (2.9).

5.2. Recovering positive volume fractions

In order to ensure the volume fraction remains positive, the piecewise parabolic method (PPM) explained in the Appendix was then applied to the continuity equations as a corrector. (The PPM using an upwind cell-face flux is a kind of finite volume method [19].) Thus

$$\frac{(\alpha h)_i^{n+1} - (\alpha h)_i^n}{\Delta t} + \frac{(\alpha h u)_{i+1/2}^n - (\alpha h u)_{i-1/2}^n}{\Delta x} = 0 \,, \tag{5.1}$$

where $(\alpha h u)_{i\pm1/2}^n$ is the cell-face flux.

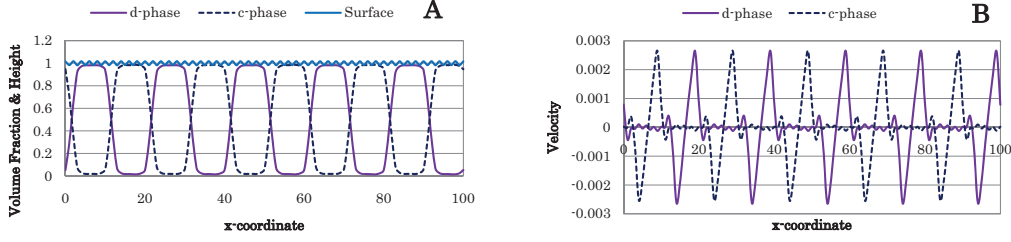Both backward and trapezoidal time stepping were tried, for the continuity equations.

Figure 2: Phase separation in the liquid film using the backward time stepping as a corrector of continuity equation restarted from the results at time 700: A, volume fractions and surface height; B, velocities at time 1300.

The invariant scheme of Eq. (4.7) and the PPM of Eq. (5.1) applied to the continuity equation involves

$$(\alpha h)_i^{n+1} = (\alpha h)_i^n + \Delta t \mathcal{L}^{INV}\left((\alpha h)_i^n\right), \tag{5.2}$$

$$(\alpha h)_i^{n+1} = (\alpha h)_i^n + \Delta t \mathcal{L}^{PPM}\left((\alpha h)_i^n\right), \tag{5.3}$$

where $\mathcal{L}^{INV}$ denotes the spatial finite difference of the invariant scheme, and $\mathcal{L}^{PPM}$ that of the PPM.

For backward time stepping, we have

$$(\alpha h)_i^{n+1*} = (\alpha h)_i^n + \Delta t \mathcal{L}^{INV}\left((\alpha h)_i^n\right),$$

$$(\alpha h)_i^{n+1} = (\alpha h)_i^n + \Delta t \mathcal{L}^{PPM}\left((\alpha h)_i^{n+1*}\right). \tag{5.4}$$

The volume fractions and surface height obtained at the time $t = 1300$ are shown in Fig. 2A, and the velocities in Fig. 2B. The calculation is restarted from the results of the invariant scheme at $t = 700$ in Figs. 1A and 1B. The positivity of the volume fraction is recovered using backward time stepping, but the surface oscillation becomes prominent. The minimum of the volume fractions is 0.0152, and the total variation of the surface height is 3.446. In the later stages of phase separation, the total value of the surface variation is expected to decrease, but the PPM procedure perturbed the cell-surface flux and caused a spurious oscillation.

For trapezoidal time stepping, we have

$$(\alpha h)_i^{n+1*} = (\alpha h)_i^n + \Delta t \mathcal{L}^{INV}\left((\alpha h)_i^n\right),$$

$$(\alpha h)_i^{n+1**} = (\alpha h)_i^{n+1*} + \Delta t \mathcal{L}^{PPM}\left((\alpha h)_i^{n+1*}\right),$$

$$(\alpha h)_i^{n+1} = \frac{(\alpha h)_i^n + (\alpha h)_i^{n+1**}}{2}. \tag{5.5}$$

The volume fractions and surface height at the time $t = 1300$ using trapezoidal time stepping restarted from $t = 700$ is shown in Fig. 3A, and the velocities in Fig. 3B. The volume fractions remain positive and the surface oscillation is decreased — the minimum of the volume fractions is 0.0143, and the total variation of the surface height is 0.789.
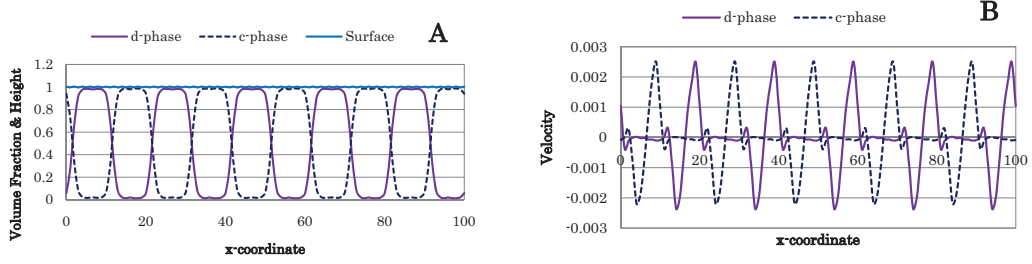
Figure 3: Phase separation in the liquid film using the trapezoidal time stepping as a corrector of continuity equation restarted from the results at time 700: A, volume fractions and surface height; B, velocities at time 1300.

The trapezoidal time stepping procedure coincides with the Heun method, a second-order Runge–Kutta method. The trapezoidal time stepping in Eq. (5.5) is shown in the form of the average of the invariant scheme in Eq. (4.7), and the backward time stepping in Eq. (5.4). Trapezoidal time stepping is strongly stable if each scheme of Eq. (5.5) is total variation diminishing (TVD) [21], whereas the invariant finite difference scheme is not. The positivity and oscillation defects of each scheme are mitigated by weight averaging — i.e. the oscillation is suppressed while positivity is maintained.

For averaged time stepping, we have

$$(\alpha h)_i^{n+1*} = (\alpha h)_i^n + \Delta t \mathscr{L}^{INV}\left((\alpha h)_i^n\right),$$
$$(\alpha h)_i^{n+1**} = (\alpha h)_i^n + \Delta t \mathscr{L}^{PPM}\left((\alpha h)_i^{n+1*}\right),$$
$$(\alpha h)_i^{n+1} = (\alpha h)_i^{n+1*} + \sigma\left((\alpha h)_i^{n+1**} - (\alpha h)_i^{n+1*}\right), \tag{5.6}$$

where σ is a constant. When $\sigma = 1/2$, Eq. (5.6) coincides with the trapezoidal time stepping in Eq. (5.5); when $\sigma = 0$, with the invariant scheme in Eq. (4.7); and when $\sigma = 1$, with the backward time stepping in Eq. (5.4).

For the case $\sigma = 0.05$, on restarting from $t = 700$ the volume fractions and surface height at the time $t = 1300$ are shown in Fig. 4A, and the velocities in Fig. 4B. The minimum of the volume fractions is 0.0017, and the overall surface variation is 0.0932. The term in the last equation of (5.6) is

$$\sigma\left((\alpha h)_i^{n+1**} - (\alpha h)_i^{n+1*}\right) = \sigma \Delta t \left(\mathscr{L}^{PPM}\left((\alpha h)_i^{n+1*}\right) - \mathscr{L}^{INV}\left((\alpha h)_i^n\right)\right),$$

which plays the role of a flux limiter.

A cold run starting from the initial condition using the averaged time stepping was performed with time step width 10^{-4}, and the other parameters the same as described above. Before time $t = 30$, only the invariant scheme was used because the PPM smoothed out the fake initial fluctuation made up of random numbers. Genuine physical fluctuation increased until $t = 30$. The volume fractions and surface height at $t = 3000$ are shown in Fig. 4C, and the velocities in Fig 4D. The minimum value of volume fractions is 0.0012, and the total variation of the surface is 0.0228.
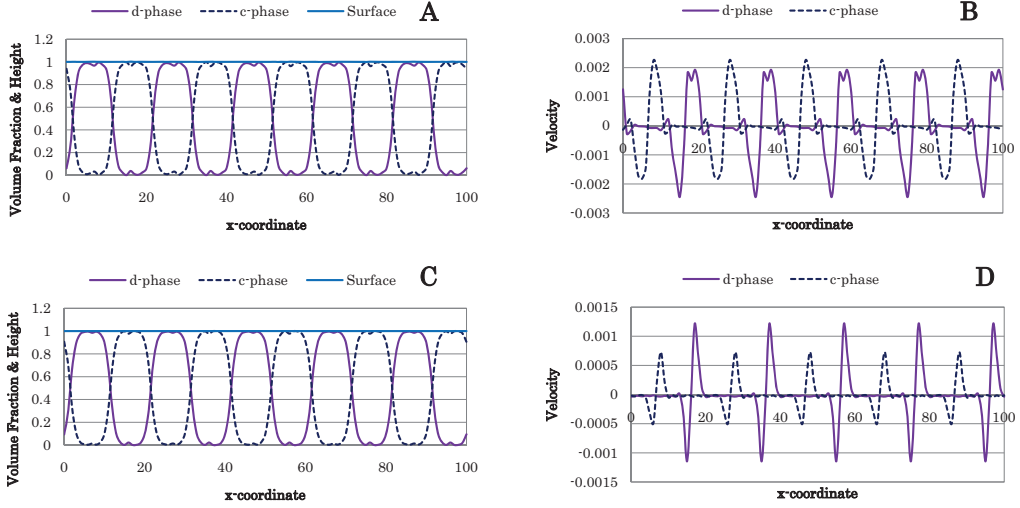
Figure 4: Phase separation in the liquid film using the averaged time stepping as a corrector of continuity equation: A, volume fractions and surface height at time 1300 restarted from the results at time 700; B, velocities at time 1300 restarted from the results at time 700; C, volume fractions and surface height of cold run at time 3000 with time step width 10^{-4}; D, velocities of cold run at time 3000.

For the cold run with $\sigma = 1$ (backward time stepping), the minimum value of the volume fraction is 0.0051 and the total surface variation is 0.2106. For the cold run $\sigma = 0$ (the invariant scheme), the minimum value of the volume fraction is -0.0039 and the total surface variation is 0.0519. The averaged time stepping shows good overall performance, from the early to the later stages.

6. Conclusions

A numerical method is constructed for the simulation of flow-driven phase separation of copolymer in a one-dimensional thin liquid film. The phenomena are modelled using two-phase shallow water equations and the Ohta–Kawasaki potential. Linear analysis of the model shows the emergence of lamellar patterns, which developed in simulations using an invariant finite difference scheme. The interface regions are highly resolved, but the positivity of the volume fraction is violated in the later stages of phase separation. Using a piecewise polynomial method (PPM) as a corrector for the continuity equations, the positivity is recovered but the PPM causes spurious oscillation of the surface. However, the surface oscillation is suppressed while maintaining positivity when averaged time stepping of the invariant scheme and the PPM are used.

Appendix

The piecewise polynomial method (PPM), as described in Ref. [19], calculates the cell-surface flux $(\alpha h u)_{i+1/2}$ as follows.

First, the cell-surface value $(\alpha h)_{i+1/2}$ is interpolated using a cubic curve

$$(\alpha h)_{i+1/2} = \frac{7}{12}\left((\alpha h)_i + (\alpha h)_{i+1}\right) - \frac{1}{12}\left((\alpha h)_{i-1} + (\alpha h)_{i+2}\right)$$

through the points $(\alpha h)_{i-1}$, $(\alpha h)_i$, $(\alpha h)_{i+1}$, $(\alpha h)_{i+2}$. The distribution of αh in a cell is assumed to be parabolic — i.e.

$$\phi(\xi) = a_0 + a_1\xi + a_2\xi^2 ,$$

where ϕ stands for αh and $\xi = (x_{i+1/2} - x)(x_{i+1/2} - x_{i-1/2})$.

In the case of $u_{i+1/2} > 0$, the coefficients of the parabola such that

$$\phi_0 = \phi(0) = (\alpha h)_{i+1/2}, \ \ \phi_1 = \phi(1) = (\alpha h)_{i-1/2}, \ \ \bar{\phi} = \int_0^1 \phi(\xi)d\xi = (\alpha h)_i$$

are $a_0 = \phi_0$, $a_1 = -4\phi_0 - 2\phi_1 + 6\bar{\phi}$, $a_2 = 3\phi_0 + 3\phi_1 - 6\bar{\phi}$.

The flux passing through the cell face at $x_{i+1/2}$ is

$$(\alpha h u)_{i+1/2} = u_{i+1/2}\int_0^{\Delta\xi}\phi(\xi)d\xi/\Delta\xi = u_{i+1/2}\left(a_0 + \frac{\Delta\xi}{2}a_1 + \frac{\Delta\xi^2}{3}a_2\right) ,$$

where $\Delta\xi = u_{i+1/2}\Delta t/\Delta x$.

When $u_{i+1/2} < 0$, we use $\xi = (x_{i+1/2} - x)(x_{i+1/2} - x_{i+3/2})$, $\Delta\xi = -u_{i+1/2}\Delta t/\Delta x$ and $\phi_0 = \phi(0) = (\alpha h)_{i+1/2}$, $\phi_1 = \phi(1) = (\alpha h)_{i+3/2}$, $\bar{\phi} = \int_0^1 \phi(\xi)d\xi = (\alpha h)_{i+1}$.

The parabola $\phi(\xi)$ is modified according to the following rules for monotonicity preservation.

Rule 1. The value at the cell surface must lie within the range of the adjacent cell values — i.e.

$$(\alpha h)_{i+1/2} = \min\left((\alpha h)_{i+1/2}^{max}, \max\left((\alpha h)_{i+1/2}^{min}, (\alpha h)_{i+1/2}\right)\right) ,$$

where $(\alpha h)_{i+1/2}^{min,max} = \min, \max((\alpha h)_i, (\alpha h)_{i+1})$. The right-hand term $(\alpha h)_{i+1/2}$ is the interpolated value and the left-hand term is the modified value.

Rule 2. The parabola must not have the apex in the cell.

However, if Rule 2 is broken, then we require

Rule 2-1. If $\left(\bar{\phi} - \phi_0\right)\left(\bar{\phi} - \phi_1\right) > 0$, then ϕ is set to be a constant value $\phi(\xi) = \bar{\phi}$.

or

Rule 2-2. A new parabola is constructed, moving the apex to one of the cell faces.

If $\left|\phi_1 - \bar{\phi}\right| < \left|\phi_0 - \bar{\phi}\right|$, the apex moves to the cell face of $\xi = 1$; $a_0 = -2\phi_1 + 3\bar{\phi}$, $a_1 = 6\phi_1 - 6\bar{\phi}$, $a_2 = 3\bar{\phi} - 3\phi_1$, or else to the cell face of $\xi = 0$; $a_0 = \phi_0$, $a_1 = 0$, $a_2 = 3\bar{\phi} - 3\phi_0$.

References

[1] R.A. Segalman, Patterning with block copolymer thin films, Materials Science and Engineering R48 (2005) pp. 191-226.

[2] M. Doi, A. Onuki, Dynamic coupling between stress and composition in polymer solutions and blends, J. Phys. II France 2 (1992) pp. 1631-1656.

[3] H. Tanaka, Viscoelastic model of phase separation, Phys. Rev. E56 (1997) 4451-4462.

[4] H. Yasuda, Two-phase shallow water equations and phase separation in thin immiscible liquid films, J. Sci. Comput. 43 (2010) pp. 471-487.

[5] T. Ohta, K. Kawasaki, Equilibrium morphology of block copolymer melts, Macromolecules 19 (1986) pp. 2621-2632.

[6] M. Ishii, Thermo-Fluid Dynamics Theory of Two-Phase Flow, Eyrolles, Paris, 1975.

[7] D. Gidaspow, Multiphase Flow and Fluidization, Academic Press, San Diego, 1994.

[8] J.N. Israelachvili, Intermolecular and Surface Forces, Academic Press, London, 1992.

[9] L.M. Pismen, Nanoscale effects in mesoscopic films, In: A.A. Golovin, A.A. Nepomnyashchy (Eds.), Self-Assembly, Pattern Formation and Growth Phenomena in Nano-Systems, Springer, Amsterdam, 2006, pp. 167-193.

[10] K. Kawasaki, Nonequilibrium and Phase Transition, Asakura, Tokyo, 2000. (in Japanese)

[11] T. Hashimoto, M. Shibayama, H. Kawai, Domain-boundary structure of styrene–isoprene block copolymer films cast from solution. 4. Molecular-weight dependence of lamellar microdomains, Macromolecules 13 (1980) pp. 1237-1247.

[12] I. Ohnishi, Y. Nishiura, M. Imai, Y. Matsushita, Analytical solutions describing the phase separation driven by a free energy functional containing a long-range interaction term, Chaos 9 (1999) pp. 329-341.

[13] V.S. Vladimirov, Methods of the Theory of Generalized Functions, Taylor & Francis, London, 2002.

[14] R. Choksi, M.A. Peletier, J.F. Williams, On the phase diagram for microphase separation of diblock copolymers: An approach via a nonlocal Cahn-Hilliard functional, SIAM J. Appl. Math. 69 (2009) pp. 1712-1738.

[15] N.N. Yanenko, Y.L. Shokin, On the group classification of the difference scheme for systems of equations in gas dynamics, In: M. Holt (Ed.), Lecture Notes in Physics 8, Springer, Berlin, 1971, pp. 3-17.

[16] N.N. Yanenko, Y.L. Shokin, Schemas numeriques invariant de groupe pour les equations de la gas, In: H. Cabannes, R. Temam (Eds.), Lecture Notes in Physics 18, Springer, Berlin, 1973, pp.174-186.

[17] R.J. LeVeque, Finite Volume Method for Hyperbolic Problems, Cambridge University Press, Cambridge, 2002.

[18] J.K. Dukowics, J.D. Ramshaw, Tensor viscosity method for convection in numerical fluid dynamics, J. Comput. Phys. 32 (1979) pp. 71-79.

[19] P.N. Blossey, D.R. Durran, Selective monotonicity preservation in scalar advection, J .Comput. Phys. 227(2008) pp. 5160-5183.

[20] P.M. Chaikin, T.C. Lubensky, Principles of Condensed Matter Physic, Cambridge University Press, Cambridge, 1995.

[21] S. Gottlieb, C.-W. Shu, Total variation diminishing Runge–Kutta schemes, Math. Comp. 67 (1998) pp. 73-85.